Super-Sensitive and Visibility-Enhanced Imaging with NOON States for Birefringent and Isotropic Samples

Shuang-Yin Huang(黄双印)[1,2], Han-Bin Xi(席寒冰)[1,2], Jing Gao(高菁)[1,2], Jing Wang(王晶)[1,2], Wen-Zheng Zhu(朱文正)[1,2], Hao Li(李浩)[1,2], Chao Chen(陈超)[3], Zhi-Cheng Ren(任志成)[1,2*], Xi-Lin Wang(汪喜林)[1,2,4,5*], and Hui-Tian Wang(王慧田)[1,2,6]

[1]*National Laboratory of Solid State Microstructures and School of Physics, Nanjing University, Nanjing 210093, China*
[2]*Collaborative Innovation Center of Advanced Microstructures, Nanjing University, Nanjing 210093, China*
[3]*School of Physical Science and Technology, Ningbo University, Ningbo 315211, China*
[4]*Hefei National Laboratory, Hefei 230088, China*
[5]*Synergetic Innovation Center of Quantum Information and Quantum Physics, University of Science and Technology of China, Hefei 230026, China*
[6]*Collaborative Innovation Center of Extreme Optics, Shanxi University, Taiyuan 030006, China*

(Received 28 August 2025; accepted manuscript online 28 September 2025)

As an emerging microscopic detection tool, quantum microscopes based on the principle of quantum precision measurement have attracted widespread attention in recent years. Compared with the imaging of classical light, quantum-enhanced imaging can achieve ultra-high resolution, ultra-sensitive detection, and anti-interference imaging. Here, we introduce a quantum-enhanced scanning microscope under illumination of an entangled NOON state in polarization. For the phase imager with NOON states, we propose a simple four-basis projection method to replace the four-step phase-shifting method. We have achieved the phase imaging of micrometer-sized birefringent samples and biological cell specimens, with sensitivity close to the Heisenberg limit. The visibility of transmittance-based imaging shows a great enhancement for NOON states. Besides, we also demonstrate that the scanning imaging with NOON states enables the spatial resolution enhancement of $\sqrt{N}$ compared with classical measurement. Our imaging method may provide some reference for the practical application of quantum imaging and is expected to promote the development of microscopic detection.

DOI: 10.1088/0256-307X/42/10/100602 CSTR: 32039.14.0256-307X.42.10.100602

Quantum precision measurement utilizes the principles of quantum mechanics to achieve measurements with higher precision than classical methods. For example, using N-entangled particles can improve the precision of spatial resolution or phase measurement, with the precision reaching $1/N$ known as the Heisenberg limit. This precision is superior to the standard quantum limit of $1/\sqrt{N}$ achieved with N non-entangled particles.[1] The core of quantum precision measurement lies in breaking through classical limit, and its application fields extend from basic science to engineering technology,[2–4] especially quantum imaging.

Quantum imaging, as a significant application in the field of quantum precision measurement, uses unique quantum properties such as correlation, entanglement, superposition, and squeezed states to break through the limitations of classical imaging techniques.[5–11] Quantum imaging can achieve ultra-high resolution, ultra-sensitive detection, and anti-interference imaging in scenarios where classical methods struggle, thus showing great potential in many fields. For example, Ghost imaging utilizes the correlation properties of photon pairs to reconstruct images without directly detecting the light reflected/transmitted by objects.[12–14] It is particularly suitable for imaging through obstacles, demonstrating unique advantages in remote sensing.[15,16] Quantum entanglement-based imaging can significantly improve the signal-to-noise ratio in low-light environments,[17–21] enabling clear imaging even with extremely weak light source, which is crucial for astronomical observation and biological microscopy,[22–26] especially for avoiding photodamage to living cells. In addition, quantum-enhanced imaging techniques, such as these based on N-entangled particles[27–33] or squeezed light,[34,35] can break through the diffraction limit and the standard quantum limit of classical optics, providing higher spatial resolution and detection sensitivity. This makes them promising in medical diagnostics and material science, such as detecting micro-structural defects in materials and early cancer detection through high-resolution imaging of biological tissues.

Quantum-enhanced imaging based on entangled NOON states has attracted extensive attention and research,[36,37] as it can approach the Heisenberg limit in phase measurement. For example, Israel *et al.* built a quantum polarized light microscope using entangled NOON states with $N = 2$ and $N = 3$, providing phase supersensitivity beyond the standard quantum limit.[38] Ono *et al.* report a confocal-type differential interference

*Corresponding authors. Email: zcren@nju.edu.cn; xilinwang@nju.edu.cn
© 2025 Chinese Physical Society and IOP Publishing Ltd. All rights, including for text and data mining, AI training, and similar technologies, are reserved.

contrast microscope under the illumination of an entangled NOON state, obtaining a better visibility than with a classical light source.[39] Besides, Camphausen *et al.* further realized wide-field phase imaging of birefringent samples and isotropic samples with the four-step phase-shifting method through a SPAD camera.[40] Most imaging based on the NOON state focuses on improving phase sensitivity, but overlooks the fact that it also contributes to the improvement of spatial resolution.

Here we build a polarization scanning microscope based on the NOON state with $N = 2$, and realize the phase imaging of birefringent samples and transparent biological cells through the four-basis projection method. Compared with a classical light source, the phase imager achieves a sensitivity close to the Heisenberg limit, the visibility of transmittance imaging shows a great enhancement and the spatial resolution is improved by a factor of $\sqrt{2}$. Our imaging method may provide some reference for label-free imaging of transparent biological samples.

During the scanning imaging process, the scanned probe light field exhibits an obvious Gaussian distribution. Considering the spatial distribution and phase of the probe beam, a single-photon state $|\Psi_1\rangle$ with Gaussian distribution can be represented by

$$|\Psi_1(x,y,\phi)\rangle = f(x,y)\mathrm{e}^{\mathrm{i}\phi}a^{\dagger}|0\rangle,$$
$$f(x,y) = \frac{1}{\sqrt{2\pi}\,\sigma}\mathrm{e}^{-\frac{x^2+y^2}{4\sigma^2}}, \tag{1}$$

where $|0\rangle$ is a vacuum state, $a^{\dagger}$ is the creation operator of a photon, ϕ is the phase carried by a single photon and $f(x,y)$ is a 2D Gaussian function representing the spatial distribution of the probability amplitude. Furthermore, for N identical photons in the state $|\Psi_1\rangle$, the spatial distribution and phase of N photons can be expressed as the Nth tensor product of $|\Psi_1\rangle$, and the N-photon state $|\Psi_N\rangle$ can be written as

$$|\Psi_N\rangle = |\Psi_1\rangle^{\otimes N} = \frac{1}{\sqrt{N!}}F(x,y)\mathrm{e}^{\mathrm{i}N\phi}(a^{\dagger})^N|0\rangle,$$
$$F(x,y) = f^N(x,y) = \frac{1}{\sqrt{2\pi}(\sigma/\sqrt{N})}\mathrm{e}^{-\frac{x^2+y^2}{4(\sigma/\sqrt{N})^2}}, \tag{2}$$

where $F(x,y)$ represents the spatial distribution of the probability amplitude for the N-photon state. Compared to single-photon states or classical light field, the beam waist of N identical photons is reduced to $1/\sqrt{N}$, while the phase will be amplified by N times. An entangled NOON state is a two-mode state in which N photons are in a superposition where N photons are in either one mode or the other. The entangled NOON state in polarization can be described as

$$|\Psi(x,y,\phi)\rangle = \frac{1}{\sqrt{2}}F(x,y)(|N\rangle_H|0\rangle_V + \mathrm{e}^{\mathrm{i}N\phi}|0\rangle_H|N\rangle_V), \tag{3}$$

where $F(x,y)$ for the NOON state shares the same spatial distribution as the N-photon state, with the beam waist reduced to $1/\sqrt{N}$ ($\sigma \to \sigma/\sqrt{N}$), and the relative phase between the two modes can also be amplified to N times ($\phi \to N\phi$).

The corresponding experimental demonstrations for the NOON state and the single-photon state are shown in Fig. 1. In Figs. 1(a)–1(c), when scanning the focal field with an extremely narrow slit, the full width at half maximum (FWHM) of the focal spot is measured to be ∼26 μm and ∼37 μm for the NOON state and the single-photon

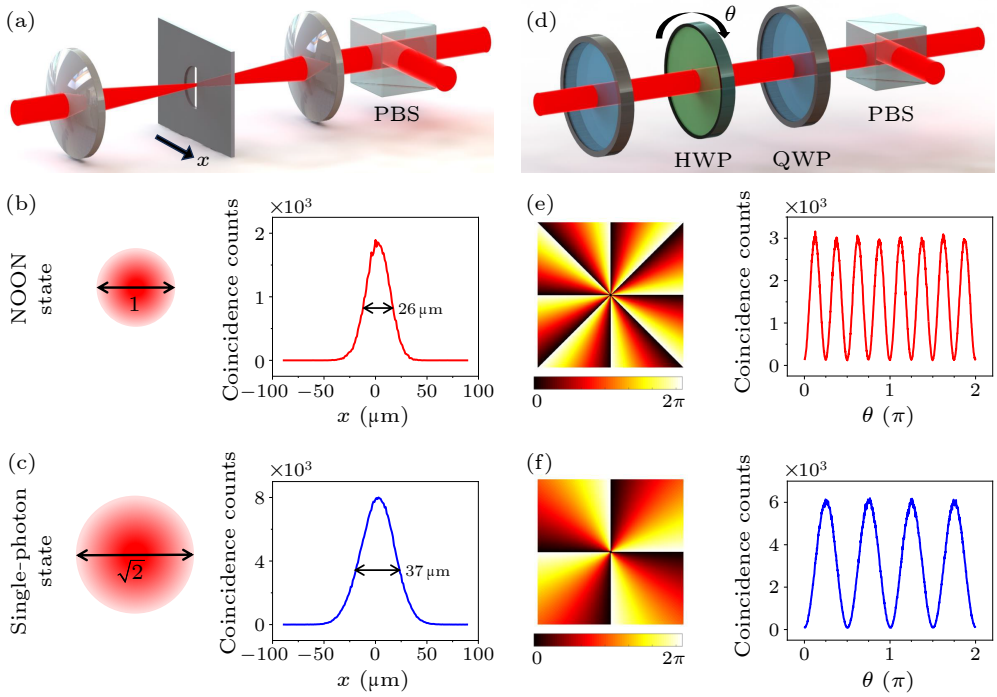

Fig. 1. Comparison of focal spot and the variation of PB phase based on the NOON state and the single-photon state. (a) Scan the focal field with an extremely narrow slit. (b) and (c) The size of the focal spot and coincidence counts under scanning with the NOON state and the single-photon state. (d) The control unit of the PB phase is composed of a HWP sandwiched by two QWPs, and the PB phase depends on the rotation angle θ of the HWP. (e) and (f) The variation of PB phase and the coincidence counts with rotation angle θ under the NOON state and the single-photon state.

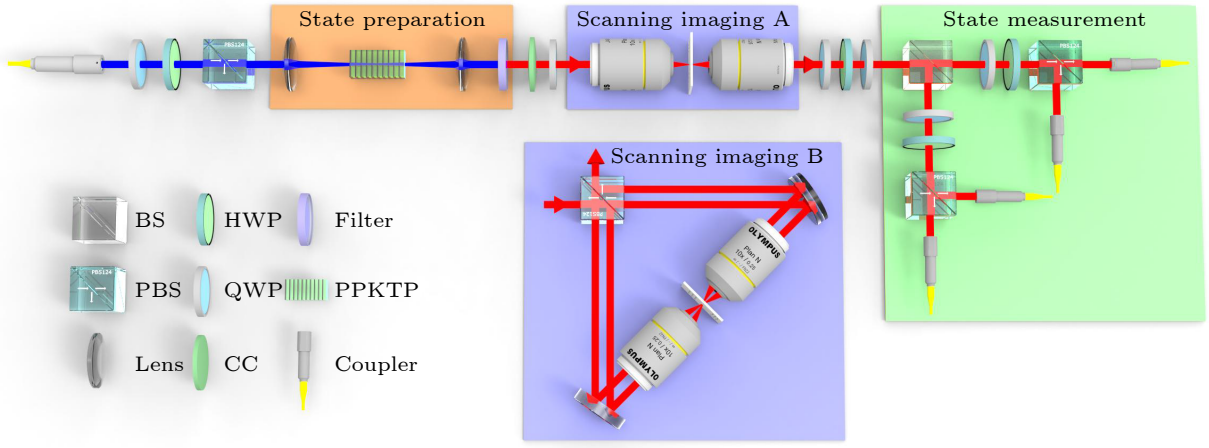

Fig. 2. Experimental setup for quantum-enhanced microscope based on the illumination of NOON states. In the "state preparation", a linearly polarized Gaussian beam at $\lambda = 780\,\text{nm}$ is incident into type-II PPKTP to create a pair of collinear photons via the SPDC process. The filter can isolate the pump beam. The extra birefringent crystal (CC) is used to compensate for the birefringent walk-off effects from the PPKTP. Passing through the QWP at 45°, the two photons will be transformed into the NOON state in the basis of $|H\rangle$ and $|V\rangle$. The "scanning imaging" mainly consists of two confocal microscope objectives (NA = 0.25, 20×) and a sample in 2D displacement stage. The "state measurement" is composed of a beam splitter (BS), following a QWP, a HWP and a PBS in each path. Finally, photons will be collected by couplers into superconducting nanowire single photon detector (SNSPD).

state, respectively. The size of the focal spot with the NOON state is $1/\sqrt{2}$ smaller than that with the single-photon state. The Pancharatnam–Berry (PB) phase related to polarization is measured, as shown in Figs. 1(d)–1(f). The measured coincidence count for the NOON state (red line) exhibits a cosine variation with the rotation angle θ of the half-wave plate (HWP), with a period of 45°. While for the single-photon, the period doubles to 90°. We find that when the HWP rotates a circle, the PB phase varies from 0 to 8π for the NOON state while from 0 to 4π for the single-photon state.[41] Clearly, the phase can be amplified by 2 times under the NOON state with $N = 2$. The experimental results are in good agreement with the theory mentioned above. For a polarization scanning microscope based on the NOON state, the NOON state can obtain smaller focal spot and achieve higher spatial resolution. In addition, the phase will be amplified by N times with sensitivity beyond the standard quantum limit.

Our microscope system is shown in Fig. 2. A 1 W quasi-monochromatic continuous-wave laser with a wavelength of $\lambda = 780\,\text{nm}$ and a narrow linewidth of 50 kHz is incident into a periodically poled potassium titanyl phosphate (PPKTP) crystal to create a pair of collinear photons via the spontaneous parametric down-conversion (SPDC) process. The PPKTP with a length of 7.5 mm is kept at 22 ℃ for the degenerate wavelength of 1560 nm. After compensating birefringent walk-off effects and passing through the quarter-wave plate (QWP) at 45°, the two photons in $|H\rangle$ and $|V\rangle$ will be transformed into the NOON state in polarization [see supplementary materials (SM) for details] as

$$|\Psi\rangle_{\text{in}} = \frac{1}{\sqrt{2}} F(x,y)(|2\rangle_H|0\rangle_V + |0\rangle_H|2\rangle_V). \tag{4}$$

For the generated NOON state, it will serve as the illumination light source for the microscope system, which includes two parts: A and B. Scanning imaging A is used for the imaging of birefringent samples and mainly consists of two confocal microscope objectives. The sample is placed at the confocal plane of two objectives, and its complete imaging information is obtained by the 2D scanning. Scanning imaging B is used for non-birefringent phase samples and includes an improved Sagnac interferometer and two confocal microscope objectives. An improved Sagnac interferometer can enable H and V photons to take two different paths with lateral shift distance about 5 mm, creating two spatially separated scanning focal points and carrying different phases. It will convert non-birefringent phase samples into birefringent samples. Here, if the birefringent phase and transmittance of the measured sample are ϕ_{un} and t_{un} in the single-photon state, the emitted NOON state will become

$$|\Psi\rangle_{\text{out}} = \frac{1}{\sqrt{2}} F(x,y) t_{\text{un}}(|2\rangle_H|0\rangle_V + \mathrm{e}^{\mathrm{i}2\phi_{\text{un}}}|0\rangle_H|2\rangle_V). \tag{5}$$

For the state measurement, we propose a simple four-basis projection method for measuring phase and transmittance. We choose four different projection basis vectors, which are created by a wave plate set instead of using a spatial light modulator or a tunable phase shifter to shift the phase.[20,40] The four basis vectors for projection measurement are $|D\rangle$, $|A\rangle$, $|E\rangle$ and $|M\rangle$, which can be written in the $|H\rangle$ and $|V\rangle$ basis as $|D\rangle = \frac{1}{\sqrt{2}}(|H\rangle + |V\rangle)$, $|A\rangle = \frac{1}{\sqrt{2}}(|H\rangle - |V\rangle)$, $|E\rangle = \frac{1}{\sqrt{2}}(|H\rangle + \mathrm{e}^{\mathrm{i}\pi/4}|V\rangle)$, and $|M\rangle = \frac{1}{\sqrt{2}}(|H\rangle - \mathrm{e}^{\mathrm{i}\pi/4}|V\rangle)$. For the coincidence measurement of two photons, it will be performed under four basis vectors $|D\rangle|D\rangle$, $|D\rangle|A\rangle$, $|E\rangle|E\rangle$, and $|E\rangle|M\rangle$, respectively, which are equivalent to the phase shifts of $\{0, \pi/2, \pi/4, 3\pi/4\}$. All the four basis vectors can be realized through the combination of a QWP and a HWP, and the specific angles of these wave plates are detailed in the SM. The unknown phase Φ_{un} and transmittance T_{un} in the NOON state to be measured can be reconstructed from the coincidence counts under the four basis vectors,

and can be extracted as [20,24,42]

$$\Phi_{\rm un} = 2\phi_{\rm un} = \arg(R_{DD} - R_{DA} + {\rm i}R_{EE} - {\rm i}R_{EM}),$$
$$T_{\rm un} = t_{\rm un}^2 = \frac{1}{2}|R_{DD} - R_{DA} + {\rm i}R_{EE} - {\rm i}R_{EM}|, \quad (6)$$

where R_{DD}, R_{DA}, R_{EE}, and R_{EM} are normalized coincidence counts under four basis vectors, respectively. In order to achieve the fast imaging, we use a BS to split the NOON state into two paths and obtain R_{DD} and R_{DA} (or R_{EE} and R_{EM}) simultaneously (see SM). The phase for the NOON state is twice of that of single-photon, and the square of transmittance is equal to that of NOON state. Finally, by scanning point by point, the phase and transmittance of each point are obtained, and then the sample information can be clearly reconstructed.

We first take a q-plate as an example to demonstrate the phase imaging with the four-basis projection method. For a q-plate with $q = 2$, we scan the q-plate using the NOON state and the single-photon state, respectively. For the NOON state, the normalized coincidence counts in the four-basis projection are shown in Fig. 3(a). The birefringent phase distribution of the q-plate can be reconstructed, as shown in Fig. 3(b). For comparison, the normalized coincidence counts and the reconstructed phases for the single-photon state are shown in Figs. 3(c) and 3(d), respectively. We found that the topological charge of the spiral phase for the q-plate reconstructed from the NOON state is exactly 2 times that from the single-photon state. To further calculate the uncertainty of phase measurement, we record the coincidence counts with the PB phase varying from 0 to 2π. The uncertainty of the phase measurement can be estimated as [38,43]

$$\sigma(\phi) = \frac{\Delta P}{|\partial P/\partial\phi|}, \quad (7)$$

where P represents the probability of the measurement result and the uncertainty associated with P is $\Delta P = \sqrt{P - P^2}$. With coincidence counts for phase measurement shown in Figs. 3(e) and 3(g), the uncertainties are estimated in Figs. 3(f) and 3(h). We find that the phase uncertainty measured based on the NOON state is close to the Heisenberg quantum limit, whereas the uncertainty based on single photons only approaches the standard quantum limit. This demonstrates the capability of ultrasensitive phase measurement with the NOON state (see SM for details).

We further achieve microscopic imaging of birefringent samples and biological cell specimens under the illumination of the NOON state. Figures 4(a)–4(f) represent the microscopic imaging of birefringent resolution targets (Thorlabs Inc. R3L1S1B). The pattern of a birefringent resolution chart is typically made of birefringent materials sandwiched between glass slides. Different incident polarization states will carry different phase patterns. Using the four-basis projection method, we can reconstruct the transmittance (T) and birefringent phase of samples. Compared with imaging based on the single-photon state with same quantum resources, the imaging in the NOON state exhibits higher contrast in both phase and transmittance. The detailed comparison of transmittance and phase is shown in Figs. 4(c) and 4(f). We can find that the phase based on the NOON state is approximately twice that of the single-photon state, demonstrating a phase sensitivity beyond the standard quantum limit. The visibility of the normalized transmittance for the NOON state and single-photon state is 0.12 and 0.06, respectively, showing an obvious enhancement for the NOON state. Figures 4(g)–4(k) indicate the microscopic imaging of paramecium specimens. First, the non-birefringent biological specimens are converted into birefringent samples with an improved Sagnac interferometer. Then, the phase and transmittance of the paramecium specimen are reconstructed with the four-basis projection method. Similar to the birefringent resolution targets mentioned above,

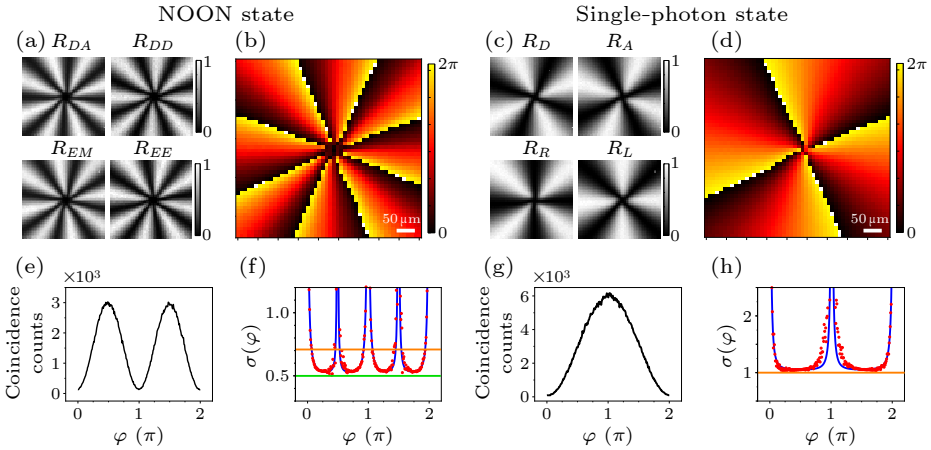

Fig. 3. Contrasting the NOON state (left row) with the single-photon state (right row) for the phase imaging of q-plate and the uncertainty estimation. (a) and (b) The normalized coincidence counts in four-basis projection and the reconstructed phase distribution of the q-plate with the NOON state. (c) and (d) For the single-photon state. (e) and (g) Variation of coincidence counts as the PB phase changes from 0 to 2π under the NOON state and the single-photon state. The PB phase is controlled by a HWP sandwiched by two QWPs. (f) and (h) The estimated uncertainty of phase measurement with the NOON state and the single-photon state. The red dots and the blue line are calculated from the coincidence counts and the corresponding fitted curves. The green line represents the Heisenberg quantum limit, while the orange lines represent the standard quantum limit.

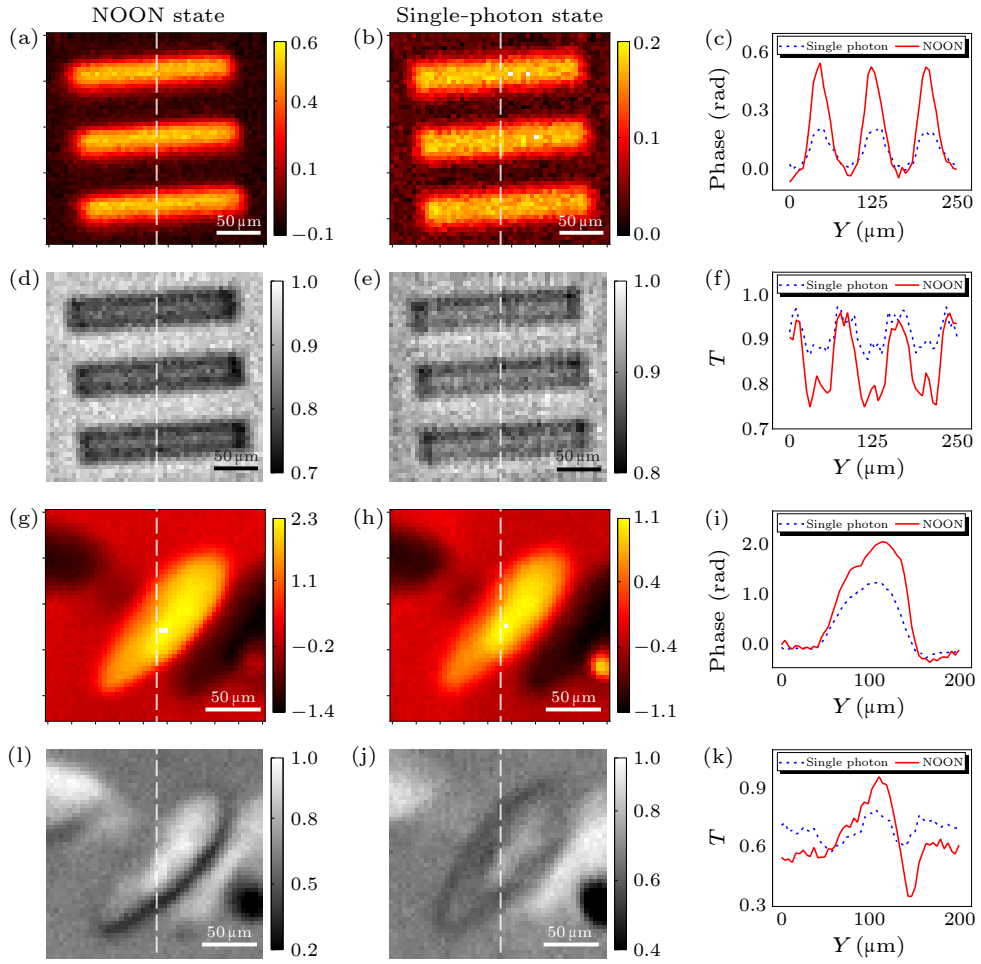

Fig. 4. Comparison of imaging between the birefringent samples and the biological cell specimens under the illumination of the NOON state and the single-photon state. (a)–(f) The microscopic imaging of birefringent resolution targets. (g)–(k) The microscopic imaging of paramecium specimens. (a) and (d), (g) and (l) The phase and the normalized transmittance (T) under the illumination of the NOON state, respectively. (b) and (e), (h) and (j) Those under the single photon state. (c) and (f), (i) and (k) The detailed comparison of phase and transmittance for the NOON state and single-photon state.

the phase based on the NOON state is approximately twice that of the single-photon state. The visibility of transmittance is 0.46 and 0.15, respectively, showing a great enhancement for the NOON state. In addition, we also introduced an obstacle on the paramecium specimen to demonstrate anti-interference imaging. The images disturbed by an obstacle are shown in the SM. The obstacle has seriously disrupted the transmittance-based imaging. However, by extracting the phase information with the four-basis projection method, we can still achieve complete imaging of the biological cell specimen, achieving anti-interference imaging.

Besides, we also use the NOON state to image amplitude-type samples, such as hair and resolution chart with a transmittance of either 0 or 1. We can directly record the coincidence counts at each scanning point. The scanning images with the NOON state and the single-photon state are shown in Fig. 5. Compared with the single-photon state, the image based on the NOON state has sharper edges. In Fig. 5(c), the lateral distance of the normalized transmittance (T) from 1 to 0 is ∼87 μm and ∼117 μm for the NOON state and the single-photon state, respectively. Besides, In Fig. 5(f), the FWHM of the slit on the resolution chart is ∼46 μm and ∼62 μm for the NOON state and the single-photon state, respectively. For the imaging with the single-photon state, we can further observe that the lateral distance of the normalized transmittance from 1 to 0 is approximately $\sqrt{2}$ times that of the NOON state. It also indicates that the resolution of scanning imaging depends on the size of the scanning focal spot. Although it does not break the standard quantum limit, it is evident that the spatial resolution based on the NOON state is significantly higher than that with a classical light source.

Throughout the development of microscopic imaging technology, researchers have been committed to continuously breaking through the resolution limit, improving imaging sensitivity, resisting interference noise, and reducing damage to samples. The quantum-enhanced microscope under the illumination of the NOON state is an important exploration towards these goals. By virtue of the unique properties of quantum mechanics, it provides new possibility for breaking through the performance bottlenecks of traditional optical microscopes. Here, we only

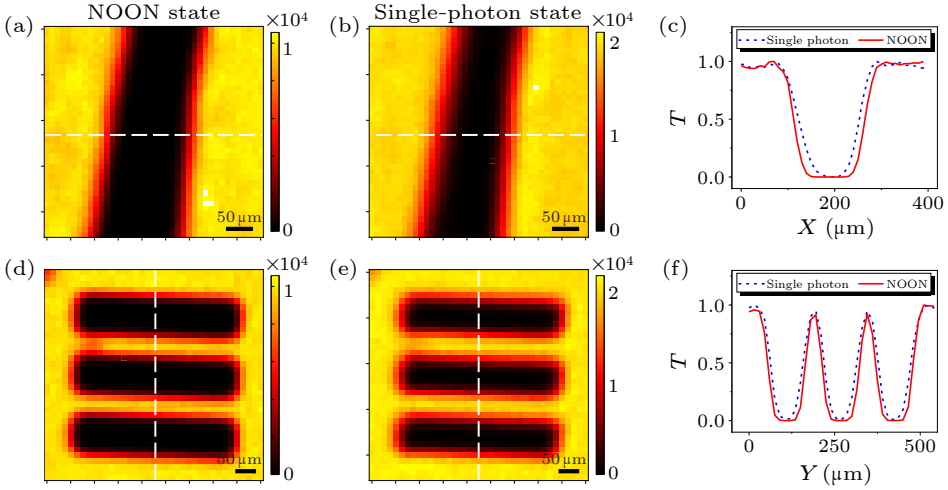

Fig. 5. Comparison of imaging between amplitude-type samples based on the NOON state and the single-photon state. (a)–(c) The imaging of a hair strand. (d)–(f) The imaging of a resolution chart with a transmittance of either 0 or 1. (a) and (d) The scanning image with the NOON state. (b) and (e) The image with the single-photon state. (c) and (f) The comparison for the normalized transmittance (T).

use a two-photon NOON state to demonstrate the characteristics of ultra-sensitivity, high-resolution, and anti-interference for quantum-enhanced microscopy. We look forward to the efficient preparation and application of NOON states with more photons.[36,44]

In summary, we have constructed and demonstrated a quantum-enhanced scanning microscope achieving ultra-sensitive detection, anti-interference imaging, and high resolution based on the entangled NOON state. We achieve the microscopic imaging of birefringent samples and biological cell samples through a simple four-basis projection method. Compared with the classical measurements, imaging with NOON state achieves a two-fold phase amplification with sensitivity approaching the Heisenberg limit, better visibility for transmittance-based imaging and the spatial resolution can be improved by a factor of $\sqrt{2}$. Our imaging technology is expected to provide some reference and assistance for the development of microscopic imaging.

Acknowledgements. This work was supported by he National Natural Science Foundation of China (Grant Nos. 12304359, 12304398, 12404382, 12234009, 12274215, and 12427808), the China Postdoctoral Science Foundation (Grant No. 2023M731611), the Jiangsu Funding Program for Excellent Postdoctoral Talent (Grant No. 2023ZB717), Innovation Program for Quantum Science and Technology (Grant No. 2021ZD0301400), Key R&D Program of Jiangsu Province (Grant No. BE2023002), Natural Science Foundation of Jiangsu Province (Grant Nos. BK20220759 and BK20233001), Program for Innovative Talents and Entrepreneurs in Jiangsu, and Key R&D Program of Guangdong Province (Grant No. 2020B0303010001).

References

[1] Demkowicz-Dobrzański R, Jarzyna M, and Kolodyński J 2015 *Prog. Opt.* **60** 345
[2] Di Giuseppe G and Vitali D 2023 *Nat. Photon.* **17** 465
[3] Taylor M A and Bowen W P 2016 *Phys. Rep.* **65** 1
[4] Zhang Z, You C, Magaña-Loaiza O S, Fickler R, León-Montiel R D J, Torres J P, Humble T S, Liu S, Xia Y, and Zhuang Q 2024 *Adv. Opt. Photon.* **16** 60
[5] Moreau P A, Toninelli E, Gregory T, and Padgett M J 2019 *Nat. Rev. Phys.* **1** 367
[6] Magaña-Loaiza O S and Boyd R W 2019 *Rep. Prog. Phys.* **82** 124401
[7] Ortolano G, Paniate A, Boucher P, Napoli C, Soman S, Pereira S F, Ruo-Berchera I, and Genovese M 2023 *Light Sci. Appl.* **12** 171
[8] Liu J and Su X 2024 *Chin. Opt. Lett.* **22** 060010
[9] Li Z P, Ye J T, Huang X, Jiang P Y, Cao Y, Hong Y, Yu C, Zhang J, Zhang Q, Peng C Z, Xu F, and Pan J W 2021 *Optica* **8** 344
[10] Xu F 2025 *Light Sci. Appl.* **14** 206
[11] Bhusal N, Hong M, Miller A, Quiroz-Juárez M A, León-Montiel R D J, You C, and Magaña-Loaiza O S 2022 *npj Quantum Inf.* **8** 83
[12] Moreau P A, Toninelli E, Gregory T, and Padgett M J 2018 *Laser Photonics Rev.* **12** 1700143
[13] Si Y, Kong L J, Li Y N, Tu C H, and Wang H T 2016 *Chin. Phys. Lett.* **33** 034203
[14] Luo K H, Huang B Q, Zheng W M, and Wu L A 2012 *Chin. Phys. Lett.* **29** 074216
[15] Li P, Chen X, Qiu X, Chen B, Chen L, and Sun B 2024 *Chin. Opt. Lett.* **22** 112701
[16] Zhao S M, Ding J, Dong X L, and Zheng B Y 2011 *Chin. Phys. Lett.* **28** 124207
[17] Defienne H, Cameron P, Ndagano B, Lyons A, Reichert M, Zhao J, Harvey A R, Charbon E, Fleischer J W, and Faccio D 2022 *Nat. Commun.* **13** 3566
[18] Xie M Y, Niu S J, Han Z Q Z, Li Y H, Chen R H, Wang X H, Gao M Y, Chen L, Song Y W, Zhou Z Y, and Shi B S 2025 *npj Quantum Inf.* **11** 57
[19] Zia D, Dehghan N, D'Errico A, Sciarrino F, and Karimi E 2023 *Nat. Photon.* **17** 1009
[20] Defienne H, Ndagano B, Lyons A, and Faccio D 2021 *Nat. Phys.* **17** 591
[21] Zhang Y, He Z, Tong X, Garrett D C, Cao R, and Wang L V 2024 *Sci. Adv.* **10** eadk1495
[22] Zheltikov A M, and Scully M O 2020 *Physics-Uspekhi* **63** 698
[23] Brown M R, Allgaier M, Thiel V, Monnier J D, Raymer M G, and Smith B J 2023 *Phys. Rev. Lett.* **131** 210801
[24] Kong L J, Zhang J, Zhang Z, and Zhang X 2025 *Laser Photonics Rev.* **19** 2401909

[25] Basset M G, Setzpfandt F, Steinlechner F, Beckert E, Pertsch T, and GräfeM 2019 *Laser Photonics Rev.* **13** 1900097
[26] Liu J, Yang Q, Chen S, Xiao Z, Wen S, and Luo H 2022 *Phys. Rev. Lett.* **128** 193601
[27] Bowen W P, Chrzanowski H M, Oron D, Ramelow S, Tabakaev D, Terrasson A, and Thew R 2023 *Contemp. Phys.* **64** 169
[28] He Z, Zhang Y, Tong X, Li L, and Wang L V 2023 *Nat. Commun.* **14** 2441
[29] Black A N, Nguyen L D, Braverman B, Crampton K T, Evans J E, and Boyd R W 2023 *Optica* **10** 952
[30] Toninelli E, Moreau P A, Gregory T, Mihalyi A, Edgar M, Radwell N, and Padgett M 2019 *Optica* **6** 347
[31] Unternährer M, Bessire B, Gasparini L, Perenzoni M, and Stefanov A 2018 *Optica* **5** 1150
[32] Cameron P, Courme B, Vernière C, Pandya R, Faccio D, and Defienne H 2024 *Science* **383** 1142
[33] Xu D Q, Song X B, Li H G, Zhang D J, Wang H B, Xiong J, and Wang K 2015 *Appl. Phys. Lett.* **106** 171104
[34] Casacio C A, Madsen L S, Terrasson A, Waleed M, Barnscheidt K, Hage B, Taylor M A, and Bowen W P 2021 *Nature* **594** 201
[35] de Andrade R B, Kerdoncuff H, Berg-Sørensen K, Gehring T, Lassen M, and Andersen U L 2020 *Optica* **7** 470
[36] Afek I, Ambar O, and Silberberg Y 2010 *Science* **328** 879
[37] Rozema L A, Bateman J D, Mahler D H, Okamoto R, Feizpour A, Hayat A, and Steinberg A M 2014 *Phys. Rev. Lett.* **112** 223602
[38] Israel Y, Rosen S, and Silberberg Y 2014 *Phys. Rev. Lett.* **112** 103604
[39] Ono T, Okamoto R, and Takeuchi S 2013 *Nat. Commun.* **4** 2426
[40] Camphausen R, Cuevas Á, Duempelmann L, Terborg R A, Wajs E, Tisa S, Ruggeri A, Cusini I, Steinlechner F, and Pruneri V 2021 *Sci. Adv.* **7** eabj2155
[41] Huang S Y, Jiang H, Ren Z C, Cheng Z M, Zhu W Z, Gao J, Liu C, Wang X L, and Wang H T 2024 *Fundam. Res.* (in press)
[42] Töpfer S, Gilaberte Basset M, Fuenzalida J, Steinlechner F, Torres J P, and Gräfe M 2022 *Sci. Adv.* **8** eabl4301
[43] Dowling J P 2008 *Contemp. Phys.* **49** 125
[44] Qin J, Deng Y H, Zhong H S, Peng L C, Su H, Luo Y H, Xu J M, Wu D, Gong S Q, Liu H L, Wang H, Chen M C, Li L, Liu N L, Lu C Y, and Pan J W 2023 *Phys. Rev. Lett.* **130** 070801